

---

## 2 Solar Phenomena and Solar wind

### 2-1 Study of Energy Build-up in Solar Flares

KUROKAWA Hiroki

To guarantee human beings to work safely and effectively in the space, the forecast for strong solar flares is indispensable. And the study of the build-up and release mechanism of the magnetic field energy, which is the source of flares, is essentially needed. This paper demonstrates which type of sunspot groups or which type of changes in the magnetic field configuration produce strong flares by showing the results obtained during the international coordinated observations in June, 2000. Our important finding is the fact that strong flares occurred right after the emergence of a strongly-twisted magnetic flux rope. We stress, therefore, the importance of further quantitative analyses of the evolution of the twisted magnetic flux rope in more details, and the importance of continuous solar observations from the space to develop the space weather research.

#### *Keywords*

Solar flare, Sunspot group, Emerging twisted flux ropes, Space weather

#### 1 Introduction

On the surface of the sun, many explosive phenomena—such as flares, prominence eruptions, and coronal mass ejections (CMEs)—unexpectedly occur, releasing strong electromagnetic waves of various wavelengths (from gamma rays and X-rays to radio waves), as well as high-energy particles and plasma clouds. The high-energy particles and powerful radiation pose a threat to space-based human activity, which will become increasingly common in the future as satellites and space stations come into more widespread practical use. Therefore, it is urgent that we elucidate the outbreak mechanisms of these phenomena to enable accurate forecasting.

Recent high-resolution observations have revealed that the main cause of the explosive phenomena on the sun is the emergence of the solar magnetic field to the surface from the internal convection zone and the sudden release of energy stored in the distorted magnetic field.

However, this research has only scratched

the surface; to progress further we need to clarify the specific details of the relationship between the development of the three-dimensional field configuration as twisted flux ropes emerge, and the formation of  $H\alpha$  filaments, flares, and CMEs. This will deepen our understanding of the process behind the energy buildup and the trigger mechanism of explosive phenomena on the solar disk, thus enabling us to forecast the occurrence of such phenomena. Furthermore, in relation to research into space weather forecasting, we expect to investigate the processes by which magnetic fields emerge repeatedly in the solar convection zone, and also how twisting of the magnetic field occurs. It is also necessary to investigate the causes of solar activity and to elucidate the origin of periodic changes in the solar magnetic field and solar irradiance.

There have been many recent observations of explosive phenomena from celestial objects outside of the solar system at levels several orders of magnitude higher than the energy accompanying solar flares; these energetic objects include flare stars, cataclysmic vari-

ables, X-ray transients, and gamma-ray bursts. It is important that we now elucidate the mechanisms behind the build-up and release of this energy, so that we may better understand the structure and evolution of the universe. The sun is the only celestial object that permits analysis of the details and dynamics of the physical structures which produce the various high-energy explosive phenomena that occur on its surface. Thus the sun serves as a laboratory in which we can investigate the basic processes of high-energy phenomena in space plasmas.

Clarifying the causes of solar flares and applying this knowledge to space weather forecasting and to a broader understanding of the universe, requires an investigation of various physical processes, including those that drive energy build-up, energy release, high-temperature plasma heating, the acceleration of non-thermal particles, and the propagation of magnetic plasma and shocks. These mechanisms are all interrelated and connected through the solar magnetic field. Obviously, research on solar flares has developed in conjunction with recent advances in observation equipment, with a growing ability to observe a wide range of wavelengths. Research using optical observations of chromospheric flares and the sunspot magnetic field, beginning from the late 1940s to the 1960s, in addition to radioastronomy and X-ray observations, such as those recorded by the recent YOHKOH satellite, have begun to reveal the physics of energy release due to magnetic reconnection in the corona. Furthermore, the movies obtained by the LASCO instrument on the SOHO satellite provide vivid and dramatic images of the corona plasma (CME) flowing out dynamically into interplanetary space. This energy originates in the magnetic flux ropes that are twisted in the convection zone as they emerge. To investigate the behavior of these flux ropes—emerging from underneath the photosphere to regions above the chromosphere and corona, and flowing out into interplanetary space—simultaneous high-resolution and high-accuracy optical observations

will be required, in addition to observations using X-rays, Extreme-Ultraviolet rays (EUVs), and radio waves.

From this perspective, this paper will present part of our research on the morphologies of emerging twisted flux ropes, focusing on recent results from coordinated international observations of the active region NOAA9026 (June 2000). We will conclude by suggesting how research on solar-flare forecasting should be conducted in the future, and the types of observation equipment that will be required.

## **2 Hida—La Palma—TRACE coordinated international observations**

We performed observations from Hida Observatory from May through June 2000, in coordination with observations carried out by the SOUP observation team of the Lockheed Martin Solar and Astrophysics Laboratory (U.S.) using the 50-cm Swedish Vacuum Solar Telescope on the Island of La Palma in West Africa's *Islas Canarias*. Observations at Hida Observatory were concluded approximately at 08-09 UT, when observations began at La Palma; these coordinated observations thus enabled continuous  $H\alpha$  image observations with unprecedented spatial resolution. In addition, the TRACE satellite also carried out observations of the same region during this period.

Fortuitously, during these coordinated observations, active region NOAA9026 appeared from the eastern edge of the sun, and as it passed near the center of the solar disk, an intense flare occurred. Of the many active regions appearing on the solar disk, the number of regions that produce X-class flares, which are defined as those seriously affecting the space environment, is considerably limited. If we look at the current cycle, 1,758 active regions designated with NOAA numbers (NOAA regions) have appeared during the five years from January 1997 through December 2001. However, only 25 of them (1.4 percent) produced X-class flares at least

once. Also, during the 11 years of the previous cycle, from 1986 through 1996, of the 3,089 NOAA regions during this period only 69 (2.2 percent) produced X-class flares (Ishii 2002). Furthermore, among these occurrences few are suitable for analysis. This is because in order to study the variations of the photospheric and chromospheric magnetic field configurations before and after the occurrence of a flare in detail, and in order to analyze the relevant energy build-up and energy release trigger mechanisms, the region needs to produce a flare near the center of the solar disk. In addition, such a region must appear during coordinated observations, and the weather must be suitable for proper operation of the high-resolution ground telescopes. If we consider the above requirements in terms of probabilities, we can conclude that the X-class flare occurrence in NOAA9026 certainly represented an extremely rare occasion.

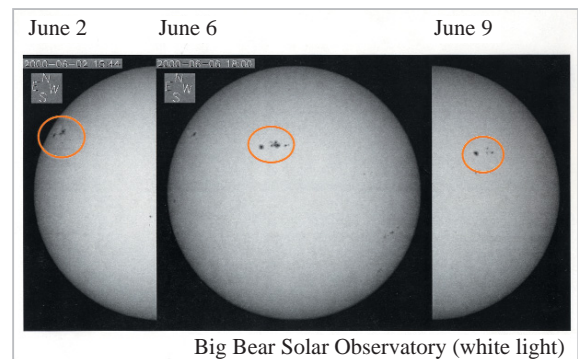
These coordinated international observations were organized by Allan Title, Tom Berger, and Richard Shine of the U.S., and, in addition to the author, by Takako Ishii, Keiji Yoshimura, Hiromichi Kozu, Taro Morimoto, Ayumi Asai, Reizaburo Kitai, and Satoru Ueno at Hida Observatory. The following results were obtained from coordinated research conducted by the author, Wang Tong Jiang, and Takako Ishii (Kurokawa et al. 2002).

The data used for this analysis are:  $H_{\alpha}$  images obtained by the domeless solar telescope at Hida Observatory;  $H_{\alpha}$  images taken by the Lockheed team; 5000Å continuum images and 1600Å images from the TRACE satellite; radial magnetograms from SOHO/MDI; and vector magnetograms obtained at Huairou Solar Observatory, Beijing Astronomical Observatory.

### 3 Development and sudden decay of active region NOAA9026

Fig.1 shows the passage of the NOAA9026 region over the solar disk. We can see from this figure that it passed close to

the center of the solar disk from June 6 to 7, when it developed most significantly, producing intense flare activity.



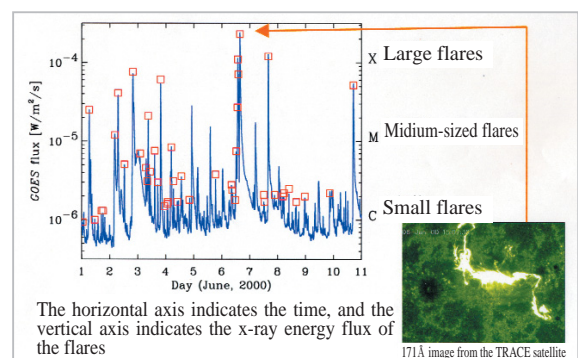
**Fig.1** Heliographic passage of the active region NOAA9026

Fig.2 shows the variation of the soft X-ray flux recorded by the GOES satellite from June 1 to 11 as this region passed across the solar disk. It can be seen that several intense flares occurred.

The flares that occurred in region 9026 are marked with squares.

As can also be inferred from the photographs in Fig.1, since there were no other significant active regions besides NOAA9026 during this period, most of the flares in Fig.2 originated within this region.

From June 2 to 4, this region produced five M-class flares, but no X-class flares. Significantly, after subsiding for two days, the region produced three consecutive X-class flares from June 6 to 7.



**Fig.2** Flares that occurred in the active region NOAA9026

x-ray flux recorded by the GOES satellite. The flares that occurred in the active region NOAA9026 are marked with squares.

According to the high-resolution  $H\alpha$  images observed continuously by the Domeless Solar Telescope at Hida Observatory (Fig. 3), the sunspot group was too close to the eastern edge on June 1 to investigate its structure in detail; however, from June 2 to 4 we can clearly observe two pairs of newly emerging dipole magnetic field regions and the development of the corresponding sunspot pairs. The M-class flare activity seen in Fig.2 was induced by the appearance of these newly emerging magnetic field regions. Although it is certainly important to study in detail the variation of the magnetic field configuration during this period, here we shall focus on and describe the development of the sunspot region before and after June 6, when more intense, X-class flares occurred consecutively.

Fig.3 shows the development and the decay of the active region between June 4 and June 8, including June 6. These images were taken at Hida Observatory. Here we can see that a strong magnetic shear structure developed on the magnetic neutral line of the  $\delta$ -type sunspot group from June 4 to 6, and that the magnetic neutral line rapidly rotated from

June 6 to 7. Also, by as early as June 8, the core portion of the  $\delta$ -type sunspots had already completely decayed.

As is clear from the GOES satellite data shown in Fig.1, this region produced intense consecutive flares (two X-class and two M-class) from 13 UT to 15 UT on June 6. This is characteristic of the flare activity in this region.

These flares occurred at night in Japan; however, at La Palma, where it was day time, the flares could be observed perfectly. Fig.4 shows the  $H\alpha$  images of the flares. All of these were homologous flares occurring along the strongly sheared magnetic neutral line within  $\delta$ -type sunspots.

What happened before and after this intense flare activity? What kind of changes occurred in the sunspot group or in the magnetic field configuration during this period? What happened to the emerging flux ropes to cause these changes? We will approach these problems in the following sections.

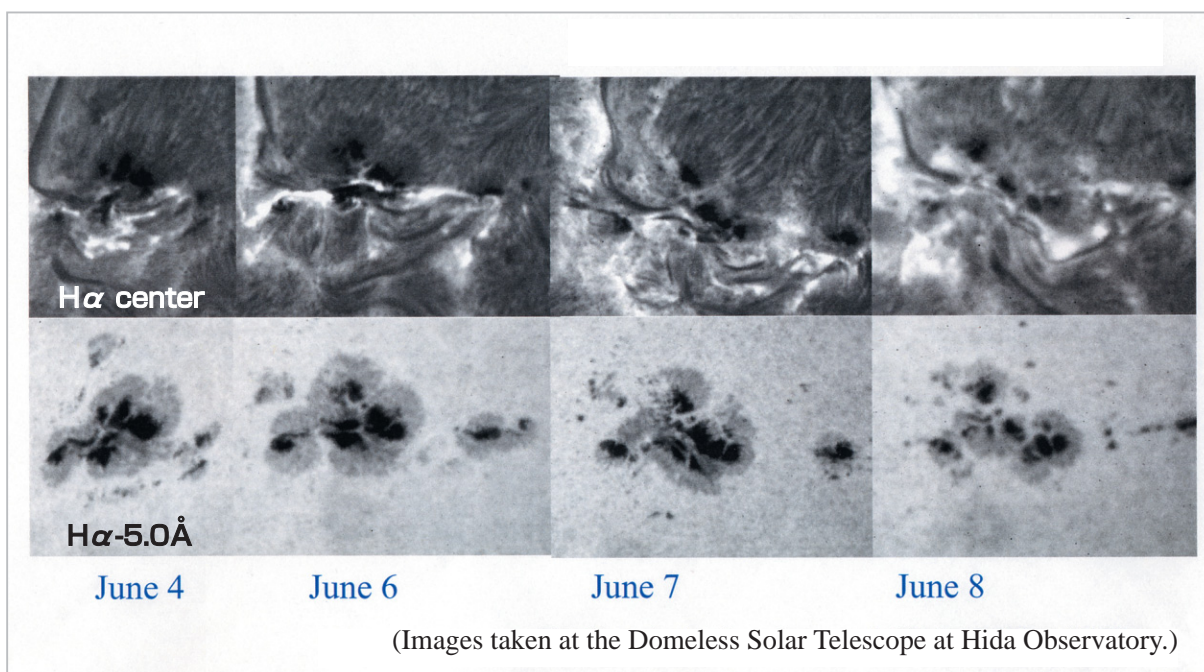


**Fig.3** Development and decay process of active region NOAA9026

These observations were made by the Domeless Solar Telescope at Hida Observatory. Note that the  $H\alpha$  filament channel (the magnetic neutral line) rapidly rotated from June 6 to 7.

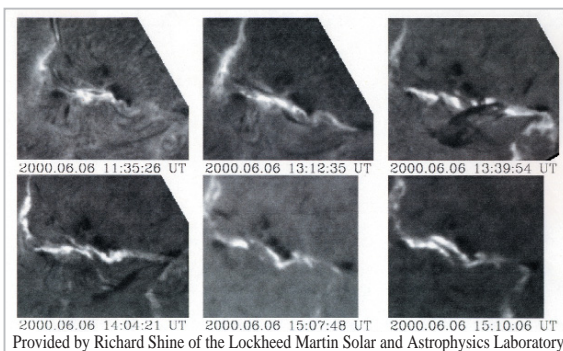


**Fig.4** Intense flares occurring consecutively along the magnetically neutral line of NOAA9026

Photographs taken by the Swedish 50-cm Vacuum Solar Telescope on the Island of La Palma.

#### 4 Proper motion of the sunspots immediately before the occurrence of the X-class flares

TRACE performed continuous observations of region NOAA9026 from June 3 through 12, providing valuable data on the development of this sunspot group. We compiled the observed 5000Å images into a movie in order to study the proper motions of the group.

The analysis of this movie and of the  $H_{\alpha}$  images from Hida Observatory has revealed the following with respect to the growth, decay, and motion of the sunspot group.

- (1) The  $\delta$ -type sunspots formed slowly in the center of region 9026 from June 3 to 6.
- (2) The magnetic shear on the neutral line of the  $\delta$ -type sunspots gradually became stronger from June 4 to 6.
- (3) The  $\delta$ -type sunspots, which had developed slowly, began to rotate and then suddenly decayed after 10 UT on June 6.
- (4) After the intense flare activity from 13 UT to 16 UT on June 6, the decay of the  $\delta$ -type sunspots proceeded further, and after another X-class flare on June 7, most of the core portion of these sunspots had disappeared by June 9.
- (5) The decay of the sunspot group from June 6 to 8 occurred over the entire sunspot group. Furthermore, the sunspots posi-

tioned at both edges of the sunspot group showed a rotational motion, suggesting interconnection. These observations strongly suggest that the sunspots were connected by a collection of flux ropes.

Fig.5 shows the sudden decay of the  $\delta$ -type sunspots, which took place immediately after 10 UT on June 6. Note that the decay of the core portion of the  $\delta$ -type sunspots was initiated between 10 UT and 11 UT.

We constructed a model for the emergence of the flux ropes that can simultaneously explain the slow growth of the  $\delta$ -type sunspot group during the earlier stage and the sudden decay in the later stage, in addition to the proper motion and rotational motion of the individual sunspots described above. We will discuss this model in Chapter 6. However, first we would like to call attention to the particularly intriguing proper motion of the sunspots.

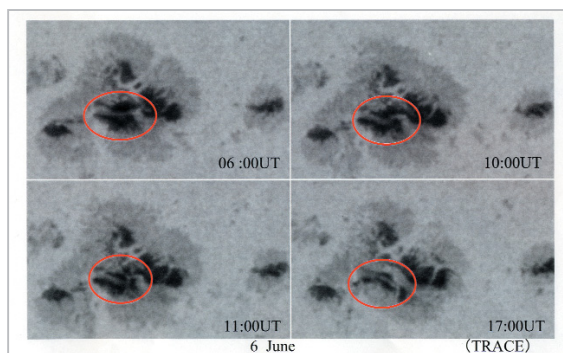


**Fig.5** Sudden decay of the  $\delta$ -type sunspots (TRACE5000Å images)

Note that the  $\delta$ -type sunspots suddenly began to decay between 10 UT and 11 UT.

Before the sudden decay of the  $\delta$ -type sunspots that induced the intense X-class flares, high-speed proper motions were observed at their eastern edge; we believe this triggered the decay of the sunspots. Fig.6 shows the temporal variation of the position of sunspot N5. "L" indicates the variation along the direction of heliographic longitude and "B" indicates the variation along the direction of heliographic latitude. In this figure, we can see that N5's high-speed motion began six hours before the occurrence of the X-class

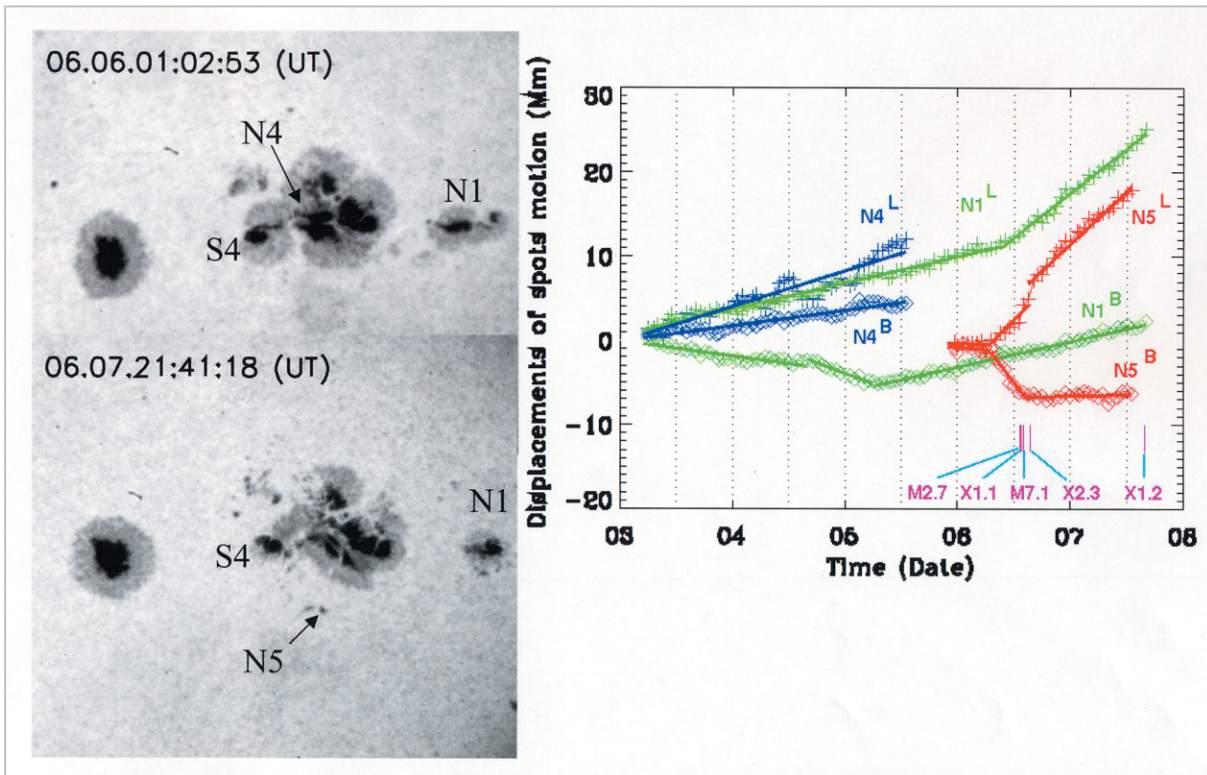


**Fig.6** High-speed motion of the sunspots, which induced the decay of the  $\delta$ -type sunspots  
 "L" indicates the motion in the direction of heliographic longitude, and "B" indicates the motion in the direction of heliographic latitude. The numbers inside the frame at the bottom indicate the classification levels of the X-ray flares, as observed by the GOES satellite. We can see that N5 and N1 began their high-speed motion about six and two hours before the occurrence of the X-class flares, respectively.

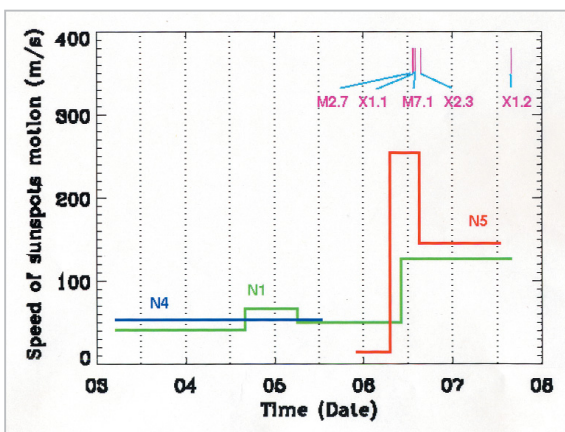
flares. It is worth noting that sunspot N1, to the west of the  $\delta$ -type sunspots, also initiated a high-speed motion at about 10 UT, when the  $\delta$ -type sunspots began to decay.

Fig.7 shows the speed of the proper motion of the sunspots shown in Fig.6. Here again, it is clearly shown that sunspots N5 and

N1 suddenly began high-speed motions about six and three hours before the occurrence of the flares, respectively.

### 5 Variation in the magnetic field immediately before the occurrence of the X-class flares

We can study the photospheric magnetic field of this region using continuous observations of the radial magnetic field by SOHO/MDI and vector magnetograms from Huairou Solar Observatory, Beijing Astronomical Observatory. First we made a movie representation of the MDI observation from June 3 through 10. As with the TRACE movie, we could clearly see the decay of the entire magnetic field configuration as the magnetic neutral line in the  $\delta$ -type sunspot region rapidly rotated after June 6. By June 10, a large part of the magnetic field in the  $\delta$ -type sunspot region had disappeared. This suggests that the



**Fig.7** Variation in speed of the proper motion of the sunspots before the occurrence of the flares

rapid rotational motion of the magnetic neutral line in the  $\delta$ -type sunspot region plays a key role in the occurrence of the X-class flares (Fig.8).

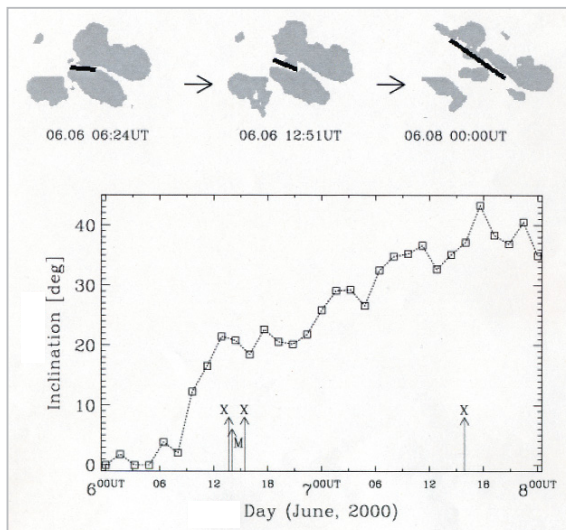


**Fig.8** Rotation of the magnetic neutral line of the  $\delta$ -type sunspots

In addition, we discovered another characteristic variation: a sudden incursion of the southern polarity region into the northern polarity region of the  $\delta$ -type sunspots immediately before the X-class flare activity on June 6. This synchronized with the rotation of the

magnetically neutral line and the development of magnetic shear, in addition to the decay of the  $\delta$ -type sunspots described in the previous section. This is a very significant observation in light of the emerging features of the flux ropes. Fig.9 shows magnetograms from Huairou Solar Observatory, Beijing Astronomical Observatory, which show the incursion of the southern polarity region into the northern polarity region.

Next, Fig.10 shows the results we obtained regarding the time variation of the radial magnetic flux using MDI data. The divisions of the region used in our measurements are shown in the MDI magnetogram on the right. For example, "p1" indicates the total northern-polarity magnetic flux within the area, and "f1" indicates the total southern-polarity magnetic flux within the area. From this figure, we can see that the magnetic flux in these three areas increased or remained constant before the intense flare activity on June 6, but that it suddenly began to decrease immediately before the flare activity.

The observed variation of the magnetic field can be summarized as follows.

- (1) The overall magnetic flux in the  $\delta$ -type sunspot region increased from June 3 to 6,

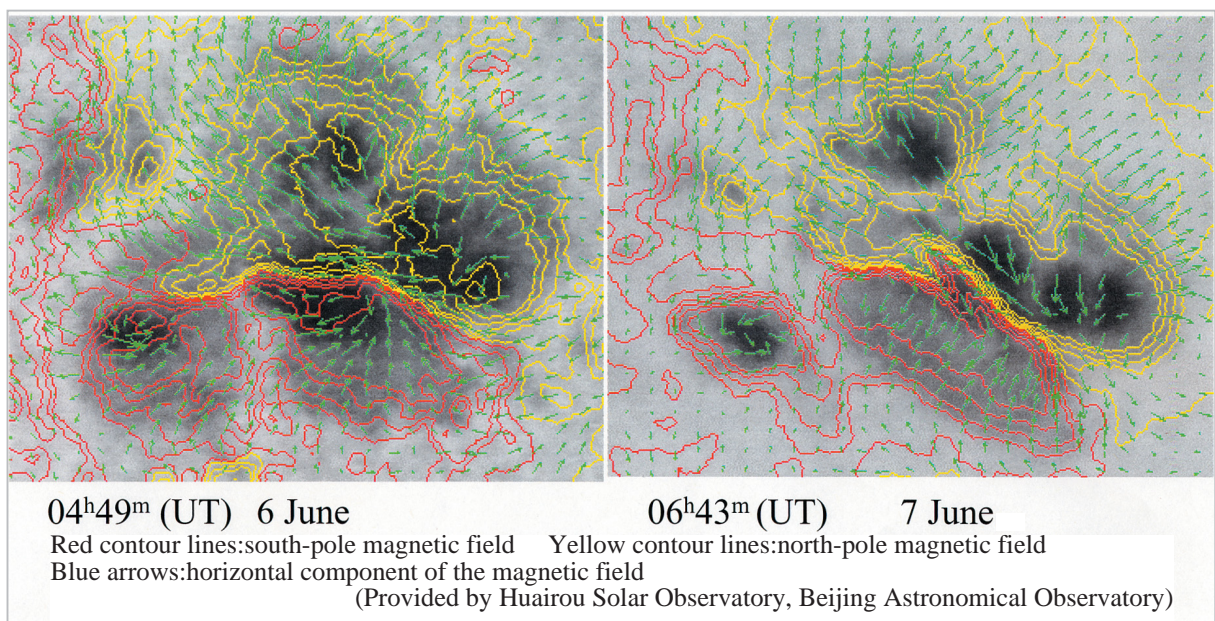


**Fig.9** Development of magnetic shear structure before the occurrence of the X-class flares  
There was an incursion into the northern-polarity magnetic field by the southern-polarity region with developed switch-back (returning) magnetic shear.

and the magnetic shear on the neutral line also became stronger.

- (2) The incursion of the southern polarity into the northern polarity began immediately before the intense flare activity on June 6; at the same time, rapid rotation of the neutral line and a sudden decrease in the magnetic flux began. By June 10, the magnetic field of the  $\delta$ -type sunspots had almost disappeared.

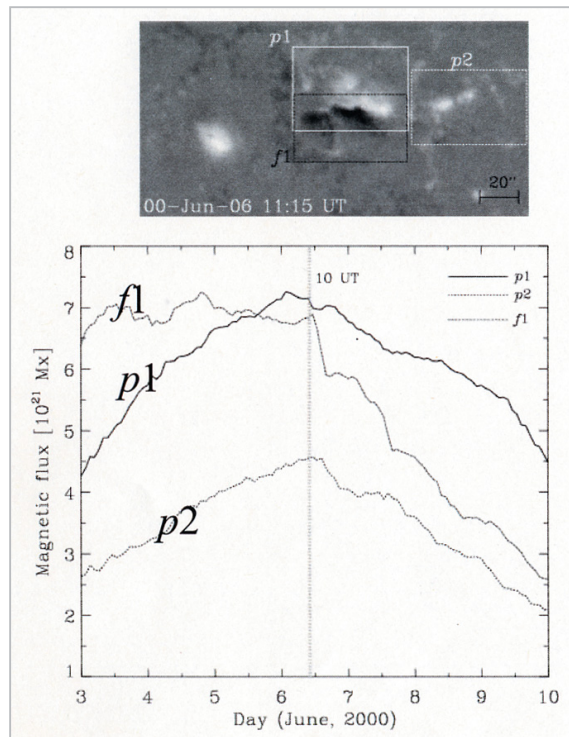


**Fig. 10** Time variation of the magnetic flux in the NOAA9026 region  
 Note that the sudden decrease in magnetic flux began immediately before the occurrence of the X-class flares.

## 6 Models for the emergence and energy release of the twisted flux ropes

From the analysis in the previous sections, we can provide an outline of the development of the NOAA9026 region, which induced intense consecutive flare activity (including three X-class flares), as follows.

- (1) A new dipole emerging flux region (EFR) appeared in the existing sunspot region, and the  $\delta$ -type sunspot group grew (June 2 to 4).

- (2) The  $\delta$ -type sunspots continued to grow, accompanied by development of a sheared magnetic structure (June 4 to the first half of June 6).
- (3) Triggered by the rapid proper motion that began in the sunspot penumbra at the eastern edge of the  $\delta$ -type sunspots, the sunspot group suddenly became unstable and began to decay. This was accompanied by rotation of the neutral line, incursion of the southern polarity into the northern polarity region, and the shear motion of the sunspots along the central line.

We will now consider models for the emerging flux ropes, which can explain this striking development of region NOAA9026. The correct model must be able to explain the rotational motion of the  $\delta$ -type sunspots, the shear motion inside these sunspots, the variation in the magnetic field, and the incursion of the southern polarity into the northern polarity, in addition to the magnitude of the proper motion and the direction of the rotational motion of the surrounding sunspots related to the rotational motion of the  $\delta$ -type sunspots.

In the following sections, we will consider two twisted flux rope models, distinguished by their respective approaches to the two types of helicities (twists): "writhe helicity" and "twist helicity." The former type of helicity is produced through twisting of the central part of the flux rope; and the latter is produced through twisting of both ends of the flux rope. The difference between the two models in question is based on the type of helicity seen as present (as the initial condition) in the convection zone.

### 6.1 Model of the emerging twisted flux rope (A) (writhe-helicity type)

As shown in Figs.11 and 12, a positive writhe helicity is applied to the central part of the flux rope. As a result, a negative twist helicity occurs over the entire flux rope due to the law of conservation of helicity. The twisted region at the center corresponds to the  $\delta$ -type sunspot, and we can assume that energy is released as the twisted flux rope loosens.

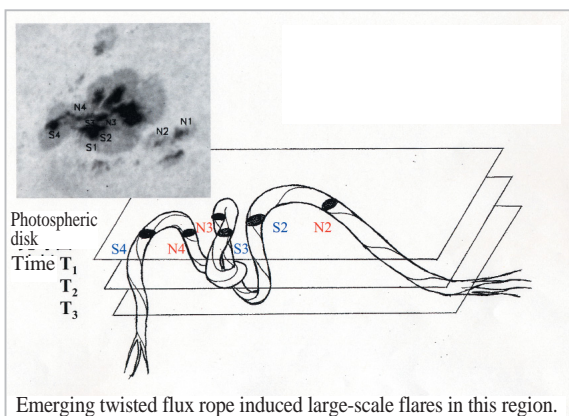


**Fig. 11** Model of the emerging twisted flux rope (A)

The positions of the photospheric disk are given by the three planes corresponding to times T 1, T 2, and T 3. In this figure, the emerging flux rope is seen as fixed, whereas the photospheric disk lowers as time passes; here the change in the formation of the positions where the flux rope breaks through the surface of the disk (at each time) corresponds to the observed motion of the sunspots.

Below is a photograph of a model we constructed to represent the twisted flux rope.

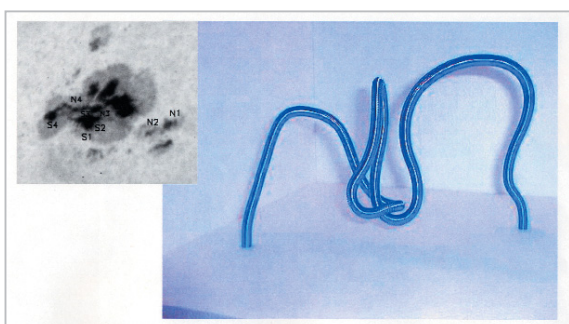


**Fig. 12** Photograph of the model of the twisted flux rope, based on the diagram in Fig. 11

Figs.11 and 12 show the three positions of the photospheric disk at times T 1, T 2, and T 3. Although the flux rope is in fact emerging from the surface, these figures treat the development over time in terms of the relative lowering of the photospheric disk. Thus the locations of the sunspots at each time T correspond to the sites where the surface of the photospheric disk is broken by the flux rope. This model can explain the growth of a strongly sheared  $\delta$ -type sunspot by the emergence of the twisted flux rope. At the same

time, it can also explain the proper motion of adjacent sunspots such as N 1, N 2, N 4, and S 4, which are connected to the  $\delta$ -type sunspot.

The flux rope continued to ascend slowly, and although the magnetic shear of the  $\delta$ -type sunspot became stronger from June 4 to 6, it was stable during this period with no extensive energy release. We note, however, that when the flux rope ascended to a certain level, it suddenly became unstable and, as shown in Fig.13, the entangled flux rope rapidly untwisted, thus initiating the observed proper motion and rotation of the sunspots, the decay of the magnetic field configuration, and the intense flare activity. This model explains the rotational motion of the sunspots well. Furthermore, it does not contradict the recent observation that negative twist helicity is dominant in active regions in the northern hemisphere (Pevtsov et al. 1995; Longcope et al. 1998). However, this model has drawbacks in its explanation of the following points: (a) the channel with the switch-back structure, as shown in Fig.9, continued to grow longer (with a narrow width) even after the X-class flare activity on June 6, and the development of the strongly sheared structure continued until the occurrence of the X-class flare on June 7; (b) it is uncertain whether it is possible to twist the central part of the flux rope locally by the Coriolis force and to create a strong writhe helicity.

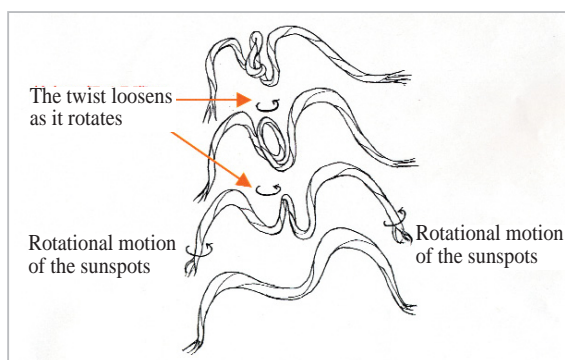


**Fig. 13** Twist-release model for the emerging flux rope

## 6.2 Model of the emerging twisted flux rope (B) (twist helicity type)

In this model, we first assume that a nega-

tive twist helicity is given to the flux rope in the convection zone. This agrees with observations of the northern hemisphere described above. This can be experimentally demonstrated by twisting both ends of a plastic tube (Fig.14). As it ascends, the strongly twisted flux rope transforms its twist helicity into writhe helicity at the center, forming a knot at this location.  $\delta$ -type sunspots are thus formed. Linton et al. (1999) and Fisher et al. (2000) have discussed this theoretical behavior of the flux rope.

Subsequently, when the flux rope passes a certain boundary within the photosphere as it ascends, a sudden transformation from twist helicity to writhe helicity due to a strong kink instability occurs. The model suggests that this phenomenon would manifest itself in the rapid rotation and decay of the  $\delta$ -type sunspots, the incursion of the south pole into the north pole, and the formation of the switch-back structure of the magnetic neutral line. A model based on this suggestion is shown in Fig.14. This model can adequately explain all of the observations (the behavior and motion of the  $\delta$ -type sunspots and the

variation of the magnetic field configuration) summarized in Chapters 4 and 5 above.

## 7 Summary

We have discussed the development of a  $\delta$ -type sunspot region which induces intense solar flare activity through the example of active region NOAA9026, which produced consecutive X-class flares. This region developed on the eastern side of the solar disk, and, as it passed close to the center of the solar disk, it produced exceptionally intense flare activity, providing us with rare and valuable data for the study of the relationship between the development of the magnetic field configuration and X-class flare activity. These observations have revealed that the sudden decay of the sunspots and the decrease in the magnetic flux began immediately before the X-class flares and that at the same time a strongly sheared switch-back-type magnetically neutral line formed, rotating in the process. All of these observations could be explained well in terms of emerging twisted flux ropes. More precisely, it seems clear that a flux rope twisted in the convection zone transformed its twist toward its central portion, forming a twisted knot (corresponding to the  $\delta$ -type sunspots) as it emerged; when it had emerged to a certain degree, it became unstable and induced consecutive X-class and M-class flares, accompanied by rapid rotational motion, shear motion, and decay of the sunspots.

Although the relationship between emerging twisted flux ropes and intense flare activity has been clarified in previous studies (Kurokawa 1987, 1989, 1996; Tanaka 1991; Ishii et al. 1998, 2000), this is the first discussion of a flux rope model that explains in detail the variation of the magnetic field configuration and the movement of sunspots observed immediately before the occurrence of X-class flares. The success of the endeavor owes a great deal to our use of the continuous data obtained by the TRACE and SOHO satellites.

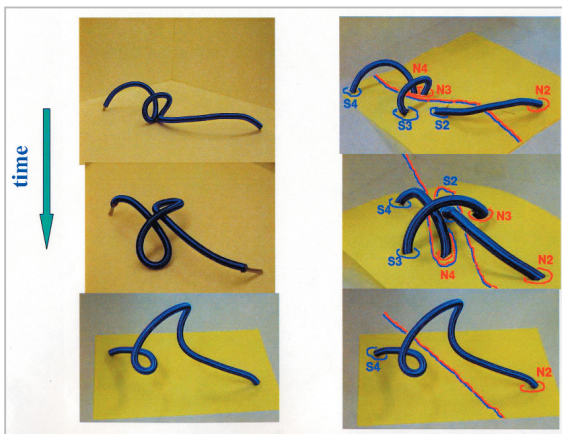


**Fig. 14** Model of the emerging twisted flux rope (B)

The twist helicity extending over the entire flux rope transforms into writhe helicity at its center as the flux rope emerges (left column). On the right we see the surface of the photosphere and where it is broken by the northern-polarity sunspots N 2, N 3, and N 4 and by the southern-polarity sunspots S 2, S 3, and S 4, in addition to the positions of the magnetic neutral line. The temporal variation seen in this model (downwards) coincides well with the observations.

The main aim of the next-generation Japanese solar observation satellite, SolarB, is to help elucidate the mechanism of coronal heating by observing minute magnetic field activity with a super-high spatial resolution of 0.2 arc seconds. However, in order to investigate the mechanisms of solar activity in the context of space weather research, another solar satellite (which will complement the use of SolarB) will be required to monitor the generation and development of active regions from a broader perspective, using a moderate spatial resolution (1 arc second) as it continuously analyzes the magnetic field activity of the entire sun. As we stated at the beginning of Chapter 2, and as the analysis of the NOAA9026 region we have presented here shows, it is important to observe phenomena as close to the center of the visible disk as possible for analysis of the magnetic field configuration in the active regions. Thus it will be significant if we can perform continuous

solar observation from point L5, since this will allow us to begin monitoring and analyzing the development of an active region in detail before it directly faces the earth. In this context we again stress the importance of space missions in making short-term and imminent space weather forecasting possible, by advancing research on the prediction of solar flares, prominence eruptions, and CMEs.

## Acknowledgments

The author would like to express his sincere thanks to the solar group members of Kwasan and Hida Observatories and to the Lockheed solar group for their cooperation in obtaining such useful observational data. He also thanks Drs. T. Ishii and T. Wang for this coanalysis of the data. Thanks are also due to Dr. D. Brooks for his improvements to the English version.

## References

- 1 Fisher, G. H., Fan, Y., Longcope, D. W., Linton, M. G., & Pevtsov, A. A.; 2000, Sol. Phys., 192, 119
- 2 Ishii, T. T., Kurokawa, H., & Takeuchi, T. T.: 1998, ApJ, 499, 898
- 3 Ishii, T. T., Kurokawa, H., & Takeuchi, T. T.: 2000, PASJ, 52, 337
- 4 Ishii, T.T., : 2002, private communication
- 5 Kurokawa, H.: 1987, Solar Phys. 113, 259
- 6 Kurokawa, H.: 1989, Space Science Review, 51, 49
- 7 Kurokawa, H.: 1996, in Magnetodynamic Phenomena in the Solar Atmosphere --- Prototypes of Stellar Magnetic Activity, ed. Y. Uchida et al., (Dordrecht: Kluwer), 185
- 8 Kurokawa, H., Wang, T., Ishii, T.T.: 2002, ApJ, 572
- 9 Linton, M. G., Fisher, G. H., Dahlburg, R. B.,& Fan, Y. : 1999, ApJ, 522, 1190
- 10 Longcope, D. W., Fisher, G. H.,& Pevtsov, A. A.: 1998, ApJ, 507



**KUROKAWA Hiroki, Ph. D.**

*Professor, Graduate School of Science,  
Kyoto University  
Director of Kwasan and Hida Observations,  
Kyoto University  
Solar Physics*